

TRACTION CHARACTERISTICS OF A ROLLING ELEMENT BEARING UNDER RAPID ACCELERATION AND IMPLICATIONS FOR AUXILIARY OPERATION IN MAGNETIC BEARING SYSTEMS

Matthew O. T. Cole and Theeraphong Wongratanaphisan
Department of Mechanical Engineering
Chiang Mai University,
Chiang Mai 50200, Thailand

ABSTRACT

The application of rolling element bearings for auxiliary operation in magnetic bearing systems is quite common, yet such operation is very different to that for which standard bearings are designed. During initial touchdown of a spinning rotor with an auxiliary bearing, rapid acceleration of the bearing inner race results in large inertial and friction forces acting on the rolling elements. Complex dynamic behavior of the bearing assembly and resulting traction forces are difficult to predict but, nonetheless, have important implications for both rotor dynamic behavior and thermo-elastic behavior of the bearing components. The aim of this work is to obtain an insight into bearing behavior by analyzing component interaction forces that would arise based on the assumption that the overall bearing traction torque is dependent only on instantaneous load, speed and acceleration. How such an analysis can be verified by experimental measurements of traction during rapid acceleration is discussed and some initial experimental results are presented. The implications for modeling and prediction of rotor-magnetic bearing system behavior during touchdown are also discussed.

INTRODUCTION

A comprehensive model of the touchdown behavior of a rotor in auxiliary bearings must incorporate a number of complex and interacting modeling elements that describe elasto-dynamic, thermo-elastic and tribological processes. A problem with such complex modeling is that the accuracy of individual model elements are difficult to verify and likewise the causes of disparities with experimental findings are difficult to pinpoint. The approach of this current work is to isolate a single subsystem of a touchdown model, namely the rolling elements of an auxiliary bearing and, through experiment and theoretical analysis, develop a model for the traction

characteristics of the rolling elements during the initial spin-up phase of the bearing operation. These traction characteristics are critical not only for determining frictional losses within the bearing but also the spin-up rate of the bearing and resulting slip-velocity at the rotor-bearing contact, both of which determine thermal conditions of bearing components. Once a reliable model for the rolling elements has been established it can then be incorporated within a complete model of an auxiliary bearing that includes inner race, sleeve, shaft and bearing support characteristics. A critical factor in the determination of auxiliary bearing life is the temperature rises due to frictional losses. Unless effective heat removal is provided then excessive temperatures will lead to lubricant deterioration, reduced fatigue resistance of contacting surfaces and reduced clearances due to thermal expansion, all of which lead to accelerated bearing failure. Thus it is important to develop analytical tools for predicting the level of heat dissipation required to maintain auxiliary bearing temperatures within tolerable limits.

There is a scarcity of reports in the current open literature that deal with behavior of auxiliary bearing components during touchdown. Previous simulation studies on rotor touchdown have focused instead on the dynamic behavior of the rotor and have therefore employed simplified models of auxiliary bearings that include stiffness and damping characteristics and simplified traction models [1-4]. A prime concern in auxiliary bearing operation is to avoid destructively high levels of rotor-bearing interaction forces. Simulation and experiment has shown that high interaction forces can occur when a rotor undergoes initial bouncing motion or if the rotor enters into a backward whirling state [5, 6]. Common conclusions are that sufficiently compliant bearing mounts and low friction rotor-bearing contact surfaces are the key to reducing peak

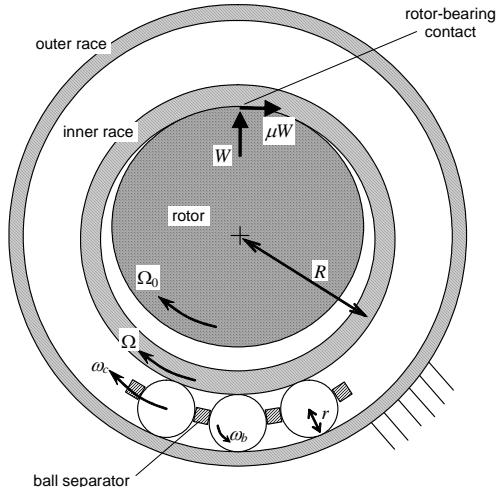


Figure 1. Auxiliary bearing components during rotor touchdown

interaction forces and avoiding backward whirl [1-6]. Other factors, such as radial clearances, rotor unbalance levels and flexural dynamics have additional influence on touchdown response and detailed studies, by simulation or experiment, would generally be required for each application [7-9]. To avoid some of the problems associated with using standard bearings for auxiliary operation some researchers have developed alternative designs, such as those based on planetary rollers or foil bearings [10].

Theoretical descriptions of rolling element auxiliary bearings have treated contact deformations at ball-race contacts combined with inner race flexibility to determine overall bearing compliance and likely stress levels during operation [11, 12]. Further work is needed if the effects of component inertia and tribology are to be accurately described. Sun also recognized the importance of thermal conditions within an auxiliary bearing and undertook theoretical calculations of temperature changes based on simulations of touchdown in a flywheel system, coupled with a one-dimensional thermal model of heat dissipation through the housing and shaft [13]. The results were used to compile performance indices for a set of varied auxiliary bearing parameters. In his study, the values adopted for bearing internal friction torque were based on empirical formulas developed for steady-speed operation [14], and therefore did not account for angular acceleration effects or transient skidding of rolling elements. This paper describes current efforts to develop models of bearing frictional forces and energy losses that are more applicable to rapidly accelerating bearings, and thus the modeling of auxiliary bearings. The first part of this paper outlines the theoretical foundation for the experimental work and proposed measurement principle, while the second part described the test rig and discusses some preliminary test data.

ROLLING ELEMENT DYNAMICS

Acceleration dependent bearing torque

The effect of rapid acceleration on bearing external forces can be deduced from a preliminary analysis considering the multi-body dynamics of an axially symmetric deep-groove bearing having N balls and a separator (Fig. 1). Referring also

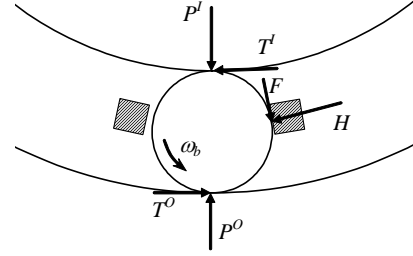


Figure 2. Contact forces acting on ball

to Fig. 2, the equation for rotational motion of the j^{th} ball (mass m_b and radius r) about its center of mass is

$$r(T_j^I + T_j^O - F_j) = I_b \dot{\omega}_{bj} \quad (1)$$

where $I_b = \frac{2}{5} m_b r^2$. The circulatory motion of each ball is determined by the separator angular velocity ω_c and so the equation for rotational motion of the ball about the bearing center is

$$RT_j^I - R(1+2s)T_j^O + R(1+s)H_j = m_b R^2 (1+s)^2 \dot{\omega}_c - I_b \dot{\omega}_{bj} \quad (2)$$

where R is the inner race radius and $s = r/R$. The equation for rotational motion of the ball separator (mass m_c) is

$$-R(1+s) \sum_j H_j = m_c R^2 (1+s)^2 \dot{\omega}_c \quad (3)$$

Equations (1) and (2) can be summed over all balls and the ball-separator interaction forces H_j eliminated using equation (3) to give

$$\mathbf{T}^I + \mathbf{T}^O - \mathbf{F} = \frac{2}{5} m_b s R \sum_j \dot{\omega}_{bj} \quad (4)$$

$$\mathbf{T}^I - (1+2s)\mathbf{T}^O = (Nm_b + m_c)R(1+s)^2 \dot{\omega}_c - \frac{2}{5} m_b s^2 R \sum_j \dot{\omega}_{bj} \quad (5)$$

Here, the bold face indicates summation over all balls e.g. $\mathbf{T}^I = \sum_j T_j^I$. Thus, expressions for the total traction force

acting on the inner and outer race respectively can be obtained as

$$2(1+s)\mathbf{T}^I = \frac{2}{5} m_b s(1+s)R \sum_j \dot{\omega}_{bj} \quad (6)$$

$$2(1+s)\mathbf{T}^O = \frac{2}{5} m_b s(1+s)R \sum_j \dot{\omega}_{bj} - (Nm_b + m_c)R(1+s)^2 \dot{\omega}_c + \mathbf{F} \quad (7)$$

If all the balls are rolling, the angular accelerations of the inner race $\dot{\Omega}$ will determine the ball spin and circulatory motion according to [14]:

$$\dot{\omega}_c = \dot{\Omega} / 2(1+s) \quad (8)$$

$$\dot{\omega}_b = \dot{\Omega} / 2s \quad (9)$$

and thus

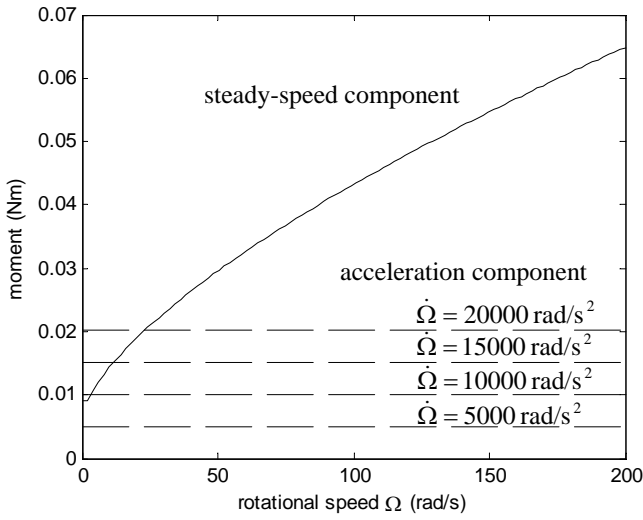


Figure 3. Predicted moment components at inner race

$$\mathbf{T}^I = \left(\frac{7}{20} Nm_b + \frac{1}{4} m_c\right) R \dot{\Omega} + \frac{1+2s}{2(1+s)} \mathbf{F} \quad (10)$$

$$\mathbf{T}^O = -\left(\frac{3}{20} Nm_b + \frac{1}{4} m_c\right) R \dot{\Omega} + \frac{1}{2(1+s)} \mathbf{F} \quad (11)$$

This analysis indicates that measurement of the reaction torques at the inner or outer race (given by RT^I and $(1+2s)RT^O$ respectively) should allow experimental determination of the mean internal friction force F/N and thus the frictional losses within the bearing due to acceleration. To calculate F would require knowledge only of the bearing parameters, the current acceleration rate $\dot{\Omega}$ and the reaction torque at either the inner or outer race. These equations also provide base-values for the traction torque developed during acceleration in a lossless bearing (for which $F = 0$). Note also that the component of T^O due to acceleration is in the opposite sense to the components due to friction, and thus it would be expected for bearing acceleration to reduce the reaction torque measured at the outer race, assuming frictional losses remain unchanged. It is also worth remarking that for a bearing without a separator the expressions for T^I and T^O have the same form as Eqs (10) and (11) except that $m_c = 0$ and the interpretation of F is altered, now being the sum of ball-ball friction forces.

A main objective of this work is thus to determine, by a combination of analysis and experimental testing, the dependency of the bearing frictional losses on the instantaneous

Table 1 Test bearing data - 6005 series

Property	Value	Unit
Inner raceway radius R	14.5	mm
Inner race mass	24.24	g
Ball radius r	3.2	mm
Ball mass m_b	1.04	g
Separator mass m_c	4.66	g
Static load capacity C_0	5850	N
Test load W	100	N

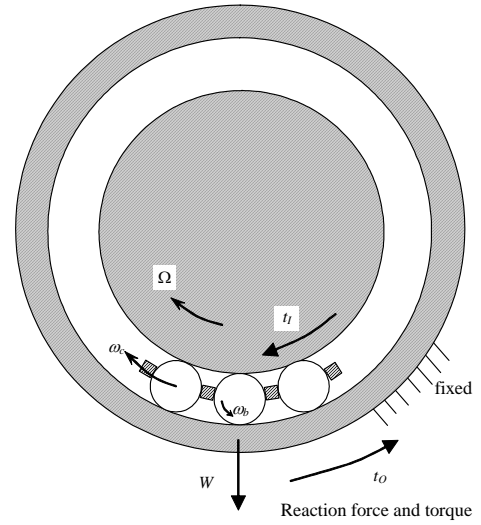


Figure 4. Traction torque measurement principle

loading and acceleration of the bearing i.e. $F(\Omega, \dot{\Omega})$ for a range of bearing types and loads.

Speed and load dependent bearing torque

For an accelerating bearing, the total moment acting on the inner and outer race from the rolling elements may be considered as a sum of steady-speed and acceleration dependent components:

$$t_I = M(\Omega, W) + RT^I(\Omega, \dot{\Omega}) \quad (14)$$

$$t_O = M(\Omega, W) + (1+2s)RT^O(\Omega, \dot{\Omega}) \quad (15)$$

Generally, the steady-speed component M can be written in terms of separate speed dependent and load dependent components: $M(\Omega, W) = M_0(\Omega) + M_1(W)$. For an oil-lubricated bearing, these two components of the resistive moment can be calculated (in Nmm) from the empirically derived formulas of Palmgren [14], which for a deep groove bearing can be written

$$M_0 \approx \begin{cases} 4.5 \times 10^{-7} f_0 (\nu \Omega)^{2/3} d_m^3, & \nu \Omega \geq 209 \\ 1.6 \times 10^{-5} f_0 d_m^3, & \nu \Omega < 209 \end{cases} \quad (16)$$

$$M_1 \approx f_1 P_1 d_m \quad (17)$$

Here, ν is the kinematic viscosity of the lubricant in mm^2/s and d_m is the mean bearing diameter in mm ($d_m \approx 2R(1+s)$). For the deep-groove ball-bearing currently considered $f_1 = 0.0009(P_0/C_0)$ and f_0 is a factor related to bearing type and lubrication method but is typically in the range 1-4. If there is no preload in the bearing then the effective load P_1 and equivalent static bearing load P_0 may both be taken as the radial rotor contact force W . C_0 is the bearing static load capacity.

Experimentally determined spin-up times for real applications vary, but are typically of the order of 0.1-1 s, which, depending on rotor speed, correspond to bearing accelerations in the range 1000-50000 rad/s^2 . Fig. 3 compares the speed dependent and acceleration dependent components of the moment t_I for various acceleration values, calculated for a test bearing using equations (14) – (17) and the data in table 1.

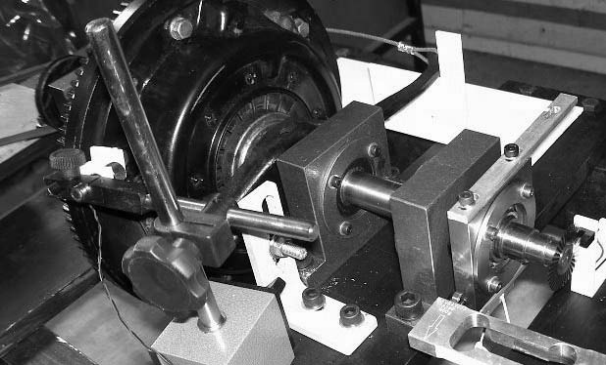


Figure 5. Auxiliary bearing test rig

These calculations assume that there are no additional frictional losses due to the acceleration i.e. $F = 0$. The data in Fig. 3 indicates that, for moderate acceleration rates, the friction component of the bearing moment would be expected to dominate over the inertial component.

Predicting inner race acceleration

The spin-up rate of the bearing inner race under auxiliary operation is dependent on the difference in traction forces arising from ball-race and rotor-bearing contacts:

$$I_I \dot{\Omega} = R_0 \mu W - t_I \quad (18)$$

Here, I_I is the moment of inertia of the inner race (and sleeve if present), μ is the coefficient for dynamic friction between the rotor and bearing and R_0 is the bore radius. It thus follows from Eq. (10) and (14) that

$$I_I \dot{\Omega} = R_0 \mu W - \left(\frac{7}{20} N m_b + \frac{1}{4} m_c\right) R^2 \dot{\Omega} - \frac{1+2s}{2(1+s)} R F(\Omega, \dot{\Omega}) - M(\Omega, W) \quad (19)$$

If $F(\Omega, \dot{\Omega})$ is known then this equation can be solved, numerically or otherwise, to find $\dot{\Omega}$ for any given W and Ω .

Experimental determination of frictional losses

It has already been shown that the reaction torque at the fixed outer race is related to internal friction and acceleration according to Eq. (11). It is therefore proposed to use the setup depicted in Fig. 4 as a means to determine the acceleration-dependent losses within an auxiliary bearing. The basic concept is to measure the reaction torque t_o during a controlled spin-up with fixed load W . The inertial component of t_o due to the known acceleration can then be subtracted in order to determine the losses.

If instantaneous accelerations cannot be determined then it is more appropriate to consider the energy losses over a complete spin-up cycle. The total work done by the inner race on the rolling elements during a complete spin-up may be obtained from Eqs (10) and (14) as

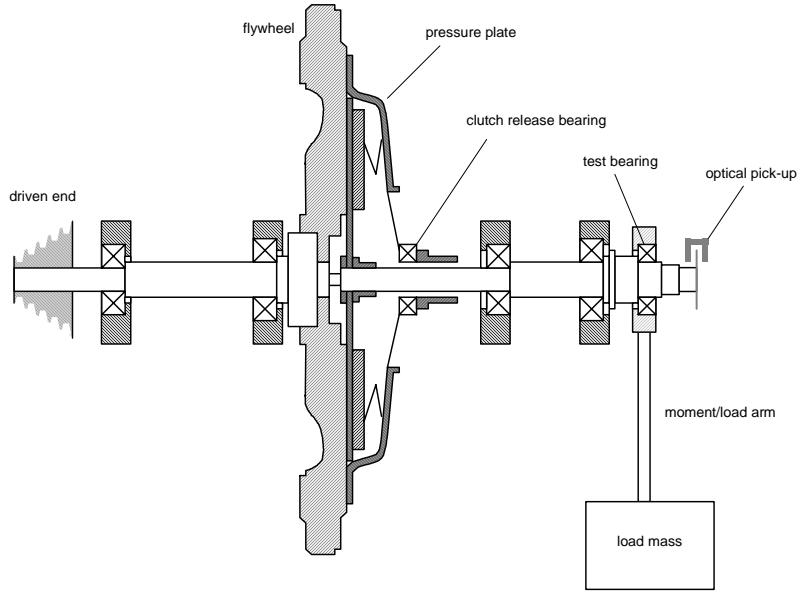


Figure 6. Auxiliary bearing test rig - schematic design

$$\int_0^{\tau} t_I \Omega dt = \underbrace{\frac{1}{2} \left(\frac{7}{20} N m_b + \frac{1}{4} m_c \right) R^2 \Omega_0^2}_{\text{kinetic energy}} + \underbrace{\frac{1+2s}{2(1+s)} R \int_0^{\tau} F(\Omega, \dot{\Omega}) \Omega dt + \int_0^{\tau} M(\Omega, W) \Omega dt}_{\text{frictional losses}} \quad (20)$$

where Ω_0 is the final bearing speed at time τ . To obtain this result, the rolling conditions (Eqs (8) and (9)) need be assumed only as final conditions. The first term on the RHS of this equation is the total kinetic energy of the bearing components, while the remaining terms correspond to the frictional energy loss, which must be dissipated as heat. From Eqs (11) and (15), this may be expressed in terms of the outer race torque as

$$\begin{aligned} \text{frictional energy losses} &= \int \frac{1+2s}{2(1+s)} F(\Omega, \dot{\Omega}) dt + \int M(\Omega, W) \Omega dt \\ &= (1+2s) \int t_o \Omega dt + \frac{1}{2} (1+2s) \left(\frac{7}{20} N m_b + \frac{1}{4} m_c \right) R^2 \Omega^2 \end{aligned} \quad (21)$$

Again, the persistent rolling condition need not be assumed to obtain this equation, except as a final state following spin-up. Importantly, this formula may be used to calculate the total energy dissipation within the bearing from measurements of Ω and the time-varying reaction torque at the outer race t_o .

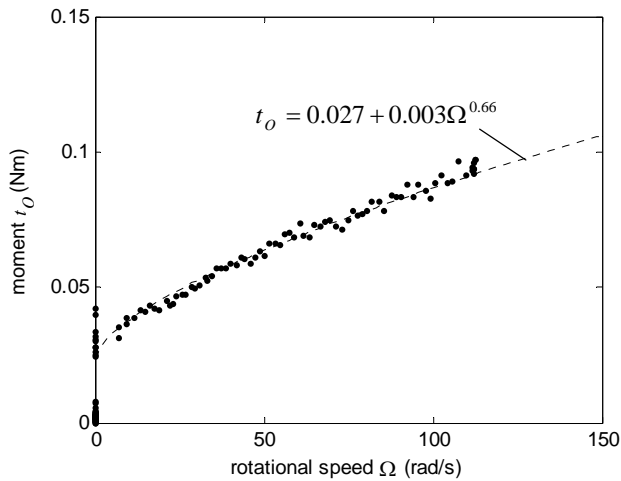


Figure 7. Bearing reaction moment t_o at steady-speed

EXPERIMENTAL METHOD

A test rig for measuring bearing conditions under rapid acceleration is currently under development (Fig. 5). The test rig consists of two shafts connected by a clutch as shown schematically in Fig. 6. The driven shaft is connected to the flywheel side of the clutch, while the bearing under test is situated on the overhung end of the non-driven shaft. During testing, the clutch is first disengaged and the flywheel is driven up to test speed by a DC motor connected through a V-belt and pulley. When the flywheel reaches test speed, the clutch is engaged, thus accelerating the test bearing to full speed. Motion of the test bearing housing can be constrained by either a vertical moment arm, to which strain gauges are mounted, or a horizontal load cell, both allowing measurement of the torque transmitted through the test bearing to the outer race during acceleration. The load on the test bearing is fixed during tests but can be changed by addition of weights suspended from the housing. The speed of the bearing is monitored by an optical pickup at the end of the shaft. The ultimate aim is to incorporate sensors to measure transients in:

- 1) bearing speed
- 2) transmitted torque
- 3) ball-pass frequency (and thus ball orbital velocity ω_c)
- 4) bearing temperatures

Data acquisition can be achieved at total sample rates up to 42 kHz using a National Instruments USB6009 device.

There are three main phenomena associated with acceleration of the bearing that will produce deviations of the torque from steady-speed values:

- 1) inertia-related torque component due to angular accelerations
- 2) friction related torque component due to acceleration
- 3) changes in torque due to ball skid $\dot{\omega}_b < \dot{\Omega}/2s$ and cage slip $\dot{\omega}_c < \dot{\Omega}/2(1+s)$
- 4) temperature related changes in clearance and lubricant properties

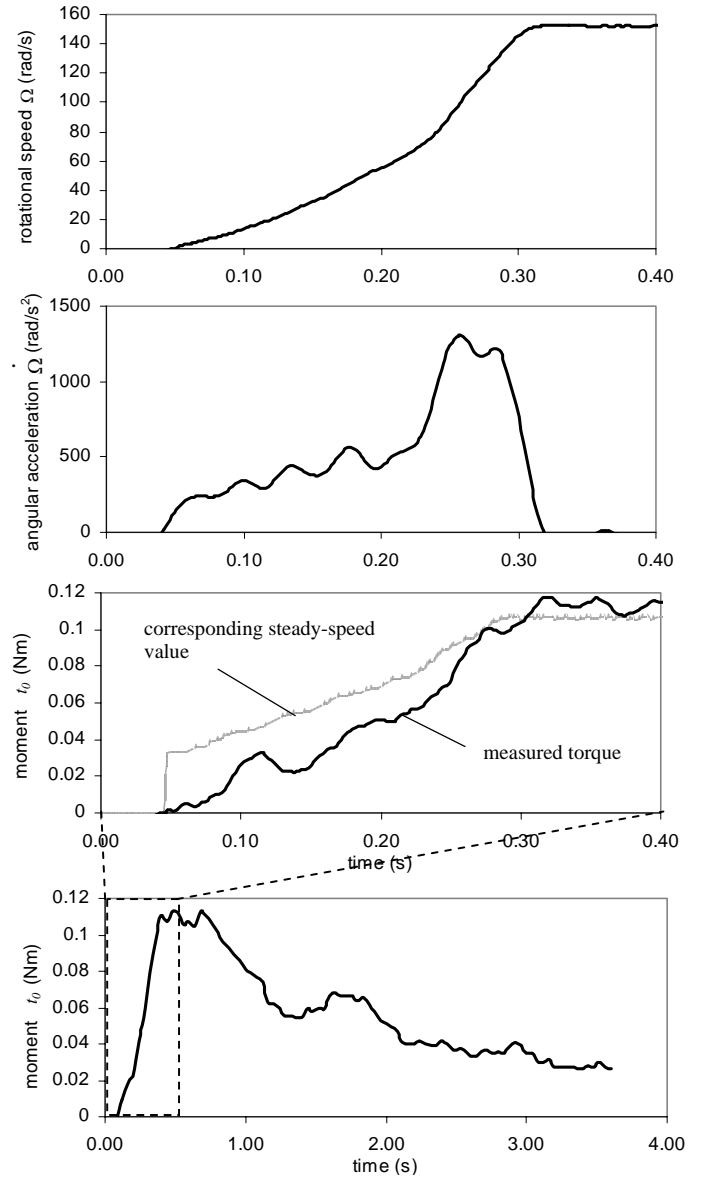


Figure 8. Speed, acceleration and measured reaction moment during bearing transient acceleration test 1

The third phenomena has not yet been discussed, but can be an issue even for steady-speed running, when ball skidding and cage slip occurs at high speeds if the bearing is not sufficiently loaded. Note that the effect of (3), like (1), is to reduce the torque acting on the outer race, while the effect of (2) is to increase the torque. All three of these phenomena have important implications for auxiliary bearing operation and bearing life and it is thus desirable to be able to quantify the degree of each effect. If ball skidding and cage slip is eliminated then it is fairly straightforward to quantify the friction and acceleration components of the measured bearing torque, by comparing with steady-speed values. However, the occurrence of phenomena (3) gives additional complications that will be discussed in the next section.

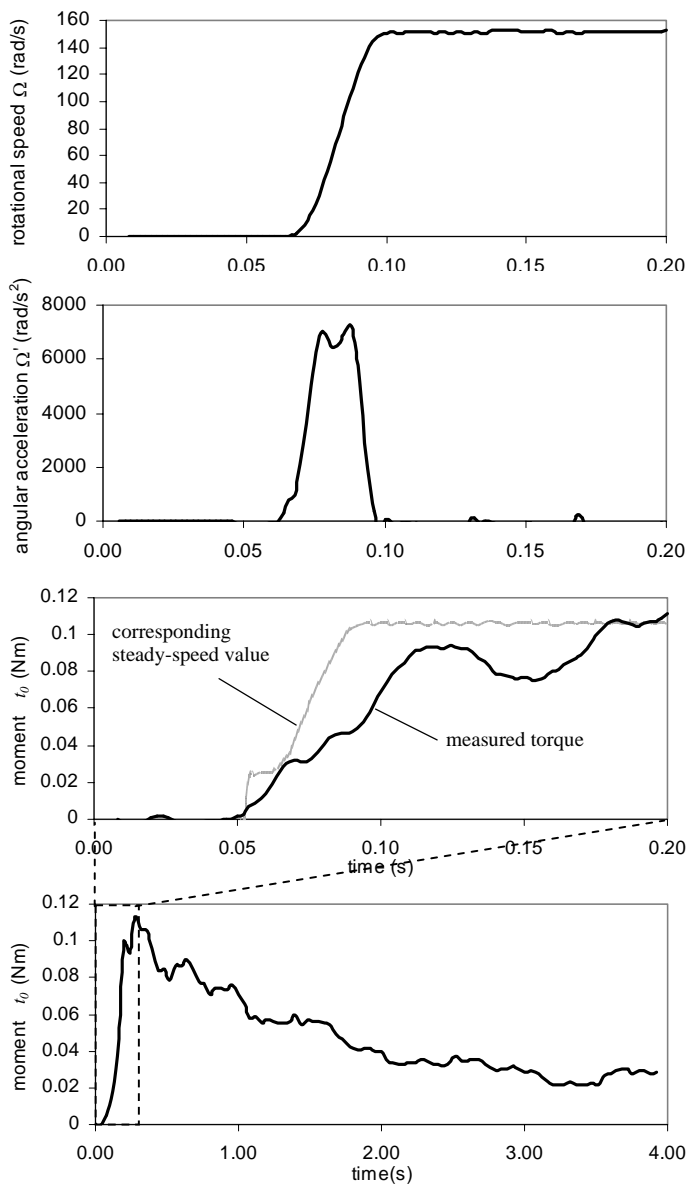


Figure 9. Speed, acceleration and measured reaction moment during bearing transient acceleration test 2

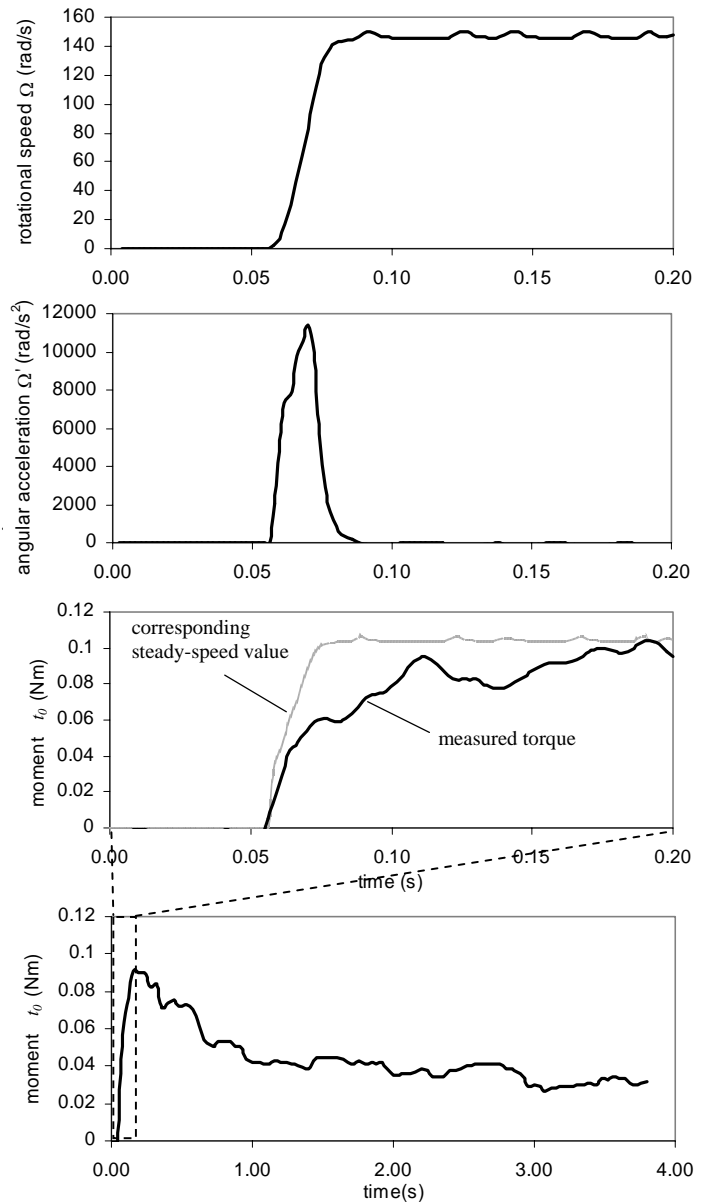


Figure 10. Speed, acceleration and measured reaction moment during bearing transient acceleration test 3

Preliminary results

To date, initial tests have been performed on a test bearing for low speed and light loading conditions. Improvements still need to be made in terms of torque measurement accuracy (particularly the dynamic response of the torque sensor) and so the current test results are interpreted qualitatively, rather than used for precise quantitative analysis. Sources of errors in the measurements of the torque acting on the outer race include:

- 1) Electrical noise and interference in the strain gauge circuit
- 2) Lateral vibration disturbances that cause deflection of the load cell, the main vibration component being synchronous with the rotational frequency

- 3) The dynamic response (i.e. settling time) of the torque sensor, which is influenced by inertia of the bearing housing and damping and compliance of the moment arm/load cell

For standard measurements of steady-speed frictional torque, errors (1) and (2) can be eliminated by time averaging, while error (3) is not an issue. However minimization of these errors is critical when rapidly changing transient torques need to be accurately determined, as is the case for the auxiliary bearing tests. An inherent difficulty with achieving this is that high sensitivity force measurements requires a compliant load cell/moment arm, but this unavoidably lowers the natural frequency and thus settling time of the sensor.

Tests were performed on an unsealed grease lubricated 6005 series bearing to determine steady-speed and acceleration behavior. The bearing was mounted with shaft and housing

interference (nominally 12 μm) sufficient to induce a small amount of preload on the balls. A degree of preload is desirable in auxiliary bearing applications in order to minimize ball skid when rotor contact forces are low. The torque measured at the outer race during a gradual coast-down from 150 rad/s is shown in Fig. 7. These results can be directly compared with the predictions in Fig. 3. The characteristics of the speed-dependent friction curve closely match the form of the empirical model, although the level of friction in the bearing is somewhat higher than the predictions, possibly due to the recent application of grease to the bearing.

The results of three tests involving torque measurements during rapid acceleration are shown in Figs. 8-10, with peak accelerations of approximately 1300, 7200 and 11500 rad/s^2 respectively. With due allowance for the inherent settling time of the torque sensor (~ 0.1 s), an underlying trend can be identified in the torque transients during the three tests. Note that for each plot of the torque response the corresponding steady-speed value has been included in the figure, calculated from the results in Fig. 7. During the initial acceleration of the inner race the torque level is significantly below the corresponding steady speed values. After an approximately 0.2-0.3 s delay, which is well after the inner race has attained full speed, the torque approaches steady-speed levels. However, the measured torque then drops over the next 3 – 4 s to levels that are significantly below steady-speed measurements.

These results were unexpected, but with consideration of the earlier analysis, an initial hypothesis can be made. The two phenomena, as previously identified, that tend to reduce the reaction torque at the outer race during acceleration are inertial effects and ball-skidding i.e. gross sliding at the ball-race contacts. The initial levels of bearing torque may be partly attributed to the acceleration of the bearing components, although according to the predictions in Fig. 3 the influence of inertial forces on total torque will be slight. The implication of the prolonged transient is that, under these test conditions, the balls and separator never attain full rolling velocities and persistent skidding of the balls must be occurring. The torque transients thus point to the conclusion that although the inner race reaches full velocity over 0.02-0.2 s, the balls and separator continue to accelerate to their final velocity over 3 – 4 s. The low level of the final steady-speed torque (as compared with the steady-speed value in Fig. 3) is also indicative that once gross sliding begins then the bearing is unable to recover from this state.

These results, though qualitative, are significant in that they appear to confirm a propensity for prolonged skidding following high acceleration conditions. Of course, in real auxiliary bearing operation the load on the bearing is time-varying and the acceleration of the inner race is dependent on the balance of traction forces transmitted from the rotor and balls, in accordance with Eq. (18). Whether ball skidding would occur over a complete rotor impact cycle must be confirmed by further testing with a full range of bearing loads and acceleration rates.

Further aims

The preliminary results that have been presented indicate that ball skidding and cage slip are important factors in the operation of the auxiliary bearing. Previous studies of skidding in bearings have generally considered angular contact bearings

under steady-speed conditions when the main contribution to ball skidding is from gyroscopic forces [15, 16]. A more relevant experimental study by MacMarsky and Hewko investigated skidding in a jet engine roller bearing. It was found that significant cage slip (down to 35% of rolling velocity) occurred under light loading conditions and over an intermediate speed range (0.5-2.5 million DN) [17]. Ball skidding tends to occur at the inner race while rolling contacts are maintained at the outer race due to centrifugal ball loading. A decrease in outer race temperature could be correlated with the degree of cage slip and attributed to the fact that rolling contacts are maintained at the outer race but at reduced velocities. However an increase in temperature was measured at the inner race where gross sliding occurs. The authors also found that cage slip could be significantly reduced with application of a high traction lubricant. Whether high traction lubricants can provide improvements in rolling element auxiliary bearing performance may be worthy of investigation.

Further development of the test rig is thus focused on the addition of sensors to measure ball velocities and bearing temperatures. With additional data on ball velocities it will be possible to more accurately determine frictional losses within the bearing and also correlate these with temperature transients.

CONCLUSIONS

This paper has described a methodology for the experimental identification of the traction characteristics of rolling element bearings under rapid acceleration. The proposed technique allows determination of the acceleration rate and frictional losses that would occur when the bearing is used for auxiliary support in a magnetic bearing system. The ultimate aim is to use the empirical data to develop improved models of auxiliary bearing dynamic behavior and thus allow more systematic methods of bearing selection. The resulting models should also enable more accurate simulation of rotor response behavior during touch-down.

The ongoing development of a test rig has been described and some of the difficulties inherent in the measurement techniques have been identified. Preliminary experimental results have been presented and indicate that significant levels of ball skidding and cage slip may be occurring in the bearing both during and after spin-up of the inner race. This has motivated further development of the identification methods to allow determination of instantaneous ball velocities and race temperatures. The outcomes of these further endeavors will form the basis of future reports.

ACKNOWLEDGEMENTS

The authors gratefully acknowledge the financial support of the Faculty of Engineering, Chiang Mai University for this work.

REFERENCES

1. Ishii, T. and Kirk, R.G., 1996, "Transient Response Technique Applied to Active Magnetic Bearing Machinery During Rotor Drop", ASME Journal of Vibration and Acoustics, Vol. 118, pp. 154-163.

2. Lawen, J.L. and Flowers, G.T., 1999, "Interaction Dynamics Between a Flexible Rotor and an Auxiliary Clearance Bearing", *ASME Journal of Vibration and Acoustics*, Vol. 121, pp. 183-189.
3. Zeng S., 2003, "Modelling And Experimental Study Of The Transient Response Of An Active Magnetic Bearing Rotor During Rotor Drop On Back-Up Bearings", *Proc. Instn Mech. Engrs, Part I*, Vol. 121, pp. 505-517.
4. Ecker, H., 1998, "Nonlinear Stability Analysis of a Single Mass Rotor Contacting a Rigid Auxiliary Bearing," *Proceedings, 5th IFToMM Conf. Rotor Dynamics*, Darmstadt, pp. 790-801.
5. Fumagalli, M., Varadi, P. and Schweitzer, G., 1994, "Impact Dynamics of High Speed Rotors in Retainer Bearings and Measurement Concepts", *4th International Symposium on Magnetic Bearings*, ETH, Zurich, pp. 239-244.
6. Fumagalli, M. and Schweitzer, G., 1996, "Measurements on a Rotor Contacting its Housing", *6th International Conference on Vibrations in Rotating Machinery*, IMechE, Oxford, pp. 779-788.
7. Kirk, R.G., 1999, "Evaluation of AMB Turbomachinery Auxiliary Bearings", *ASME Journal of Vibration and Acoustics*, Vol. 121, pp. 156-161.
8. Keogh P. S., Seow, Y-H. and Cole, M. O. T., 2005, "Characteristics of a Magnetically Levitated Flexible Rotor When In Contact With One Or More Auxiliary Bearings", *Proceedings, ASME Turbo Expo 2005*, Reno, USA, Paper No GT-2005-68583
9. Cuesta, E.N., Rastelli, V., Medina, L. U., Montbrun, N.I. and Diaz, S.E., 2002, "Non-Linear Behaviors in the Motion of a Magnetically Supported Rotor on the Catcher Bearing During Levitation Loss, an Experimental Description", *Proceeding ASME Turbo Expo 2002*, Amsterdam, Netherlands, paper GT2002-30293.
10. Swanson E.E. and Heshmat, H., 2002, "Oil-Free Foil Bearings As A Reliable, High Performance Backup Bearing For Active Magnetic Bearings", *Proceeding ASME Turbo Expo 2002*, Amsterdam, Netherlands, paper GT2002-30291.
11. Cole, M.O.T. Keogh, P.S. and Burrows, C.R., 2002, "Predictions on the Dynamic Behaviour of a Rolling Element Auxiliary Bearing for Rotor/AMB Systems", *Proceedings, Eighth International Symposium On Magnetic Bearings*, Mito, Japan, pp. 501-506.
12. Sun, G., Palazzolo, A.B., Provenza, A. and Montague, G., 2004, "Detailed Ball Bearing Model For Magnetic Suspension Auxiliary Service", *Journal of Sound and Vibration*, Vol. 269, pp. 933-963.
13. Sun, G., 2005, "Rotor Drop and Following Thermal Growth Simulations Using Detailed Auxiliary Bearing and Damper Models", *Journal of Sound and Vibration*, In press 2005.
14. Harris, T.A., 1966, "Rolling Bearing Analysis", Wiley, New York.
15. Jones, A. B. ,1959 "Ball motion and sliding friction in ball bearings", *Transactions of ASME, Journal of Basic Engineering*, Series D, Vol. 81, pp. 1-12.
16. Harris T.A., 1971, "An Analytical Method To Predict Skidding In Thrust Loaded, Angular-Contact Ball Bearings", *ASME Journal of Lubrication Technology*, Vol. 93, pp. 17-24.
17. MacMarsky, W.M. and Hewko, L.O., 1971, "Effect Of A High Traction Fluid On Skidding in a High Speed Roller Bearing", *ASME Journal of Lubrication Technology*, January, pp. 11-16.